Published OnlineFirst September 17, 2010; DOI: 10.1158/1078-0432.CCR-10-0825

Imaging, Diagnosis, Prognosis

Clinical Cancer Research

Overexpression of High-Mobility Group Box 2 Is Associated with Tumor Aggressiveness and Prognosis of Hepatocellular Carcinoma

Jung-Hee Kwon[1], Jongmin Kim[2], Jin Young Park[2], Sun Mi Hong[1], Chang Wook Park[1], Seok Joo Hong[2], Sun Young Park[2], Yoon Jung Choi[3], In-Gu Do[4], Jae-Won Joh[5], Dae Shick Kim[4], and Kwan Yong Choi[1]

Abstract

Purpose: We investigated the expression of high-mobility group box 2 (HMGB2) in patients with hepatocellular carcinoma (HCC) and its clinical effects with underlying mechanisms.

Experimental Design: *HMGB2* mRNA levels were measured in 334 HCC patients by real-time reverse transcription-PCR and HMGB2 protein levels in 173 HCC patients by immunohistochemical studies. The HMGB2 expression level was measured by Western blotting for three HCC cell lines. To clarify the precise role of HMGB2 on cell proliferation, we did *in vitro* analysis with expression vectors and small interfering RNAs.

Results: HMGB2 mRNA and protein expression were significantly higher in HCC than in noncancerous surrounding tissues ($P < 0.0001$) and showed a positive correlation ($\rho = 0.35$, $P < 0.001$). HMGB2 overexpression was significantly correlated with shorter overall survival time, both at mRNA ($P = 0.0054$) and protein level ($P = 0.023$). Moreover, *HMGB2* mRNA level was an independent prognostic factor for overall survival in a multivariate analysis ($P = 0.0037$). *HMGB2* knockdown by small interfering RNAs decreased cell proliferation, and overexpression of *HMGB2* by expression vectors diminished cisplatin- and etoposide-induced cell death.

Conclusions: Our clinical and *in vitro* data suggest that HMGB2 plays a significant role in tumor development and prognosis of HCC. These results can partly be explained by altered cell proliferations by HMGB2 associated with the antiapoptotic pathway. *Clin Cancer Res; 16(22); 5511–21. ©2010 AACR.*

Hepatocellular carcinoma (HCC) is the fifth most common cancer worldwide and the most common primary hepatic malignancy, being responsible for 80% of malignant tumors in adult livers (1). HCC is known for its endemic prevalence in Asia and Africa, and an increasing incidence of HCC is reported in Western countries (2, 3). HCC is resistant to conventional chemotherapy and is rarely amenable to radiotherapy (1), leaving this disease with no effective therapeutic options and a very poor prognosis. Although the major etiologic agents have been identified, the molecular pathogenesis of HCC remains unclear (4). It is therefore important to clarify the molecular pathogenesis of HCC and identify molecular targets to develop novel diagnostic, therapeutic, and preventive strategies.

High-mobility group box (HMGB) proteins are ubiquitous, abundant nuclear proteins and have diverse functions in the cell. HMGB1 and HMGB2 are highly conserved (with >80% amino acid identity) and have indistinguishable biological properties such as binding to DNA without sequence specificity (5–7). As an extracellular component, HMGB1 has been linked to diseases such as sepsis, arthritis, and cancer (8). HMGB1 overexpression has been reported in a variety of human cancers, including melanoma (9), pancreatic cancer, prostate cancer (10), colorectal cancer (11), and breast cancer (12). More importantly, HMGB proteins preferentially bind to cis-platinum(II)diamine-dichloride (cisplatin)–modified DNA or to misincorporated nucleoside analogues and consequently inhibit nucleotide excision repair, which could be of great value in cancer treatment (13, 14). Despite extensive characterization of the diverse roles of HMGB1 in cancer, much less is known of the signaling pathways of HMGB2, especially its relevance in carcinogenesis. Recently, the overexpression of

Authors' Affiliations: [1]Department of Life Science, Pohang University of Science and Technology, Pohang, South Korea; [2]CbsBioscience, Inc., Daejeon, South Korea; [3]Department of Pathology, National Health Insurance Corporation Ilsan Hospital, Goyang, Gyeonggi, South Korea; and Departments of [4]Pathology and [5]Surgery, Samsung Medical Center, Sungkyunkwan University School of Medicine, Seoul, South Korea

Note: Supplementary data for this article are available at Clinical Cancer Research Online (http://clincancerres.aacrjournals.org/).

J-H. Kwon and J. Kim contributed equally to this work.

Corresponding Authors: Kwan Yong Choi, Department of Life Science, Pohang University of Science and Technology, Hyoja-Dong, Pohang 790-784, South Korea. Phone: 82-54-279-2295; Fax: 82-54-279-2199; E-mail: kchoi@postech.ac.kr or Dae Shick Kim, Department of Pathology, Samsung Medical Center, Sungkyunkwan University School of Medicine, Seoul 135-710, South Korea. Phone: 82-2-3410-2764; Fax: 82-2-3410-6396; E-mail: oncorkim@skku.edu.

doi: 10.1158/1078-0432.CCR-10-0825

Published OnlineFirst September 17, 2010; DOI: 10.1158/1078-0432.CCR-10-0825

Translational Relevance

Hepatocellular carcinoma (HCC) is highly refractory to conventional chemotherapy and radiation therapy, and less than one third of patients are eligible for curative surgery. The current study showed for the first time through large-scale real-time reverse transcription-PCR and immunohistochemistry that high-mobility group box 2 (HMGB2) expression is significantly associated with prognosis of HCC patients. Moreover, *in vitro* study indicated that altered HMGB2 level affects cell proliferation as well as cisplatin- and etoposide-induced cell death. Therefore, on the basis of our findings that HMGB2 may contribute to cell survival through the antiapoptotic pathway, HMGB2 could be an important factor in determining therapeutic strategies for HCC.

HMGB proteins in rat and human HCC tissues was reported, and knockdown of HMGB2 expression in a rat HCC cell line by RNA interference reportedly inhibited cell growth (15). However, only a small number of human HCC tissues have been analyzed in relation to HMGB2 expression and the prognostic significance of HMGB2 expression remains to be elucidated.

The present study investigated the clinicopathologic significance of HMGB2 expression in a large number of HCCs by quantitative real-time reverse transcription-PCR (RT-PCR) and immunohistochemistry. Furthermore, we analyzed *in vitro* the effects of *HMGB2* knockdown on cell growth and *HMGB2* overexpression on cisplatin- and etoposide-induced cell death. Our studies suggest that HMGB2 expression has implications for predicting clinical outcome and choosing treatment modalities for HCC patients, even if the precise role of HMGB2 in tumor cell growth is as yet not entirely clear and requires further study.

Materials and Methods

Patients and tissue samples

HCC tissues and corresponding noncancerous hepatic tissues were obtained with informed consent from 350 patients who had undergone curative hepatectomy for primary HCC between 2001 and 2005 in the Department of Surgery, Samsung Medical Center in South Korea. The study protocol was approved by the Institutional Review Board of Samsung Medical Center. Complete clinical data were available in all 350 cases. The mean age of patients was 48.2 years (ranging from 20 to 80 years). All patients had adequate liver function reserve and had survived for at least 2 months after hepatectomy (median follow-up, 51.2 months; range, 2.7–95.6 months). Recurrence or death was evaluated from medical records of patients. We defined recurrence as evidence of an overt new growing mass in the remaining liver or as distant metastasis in radiologic studies including computed tomography or magnetic resonance imaging. None of the patients had received treatment prior to surgery such as transarterial chemoembolization or radiofrequency ablation. Clinicopathologic features of the 334 HCCs analyzed by RT-PCR and 173 HCCs analyzed by immunohistochemistry (157 randomly selected samples from tumors analyzed by RT-PCR and 16 additional independent cases) in the current study are summarized in Table 1. Immediately after hepatectomy, fresh tumors and background livers were partly snap-frozen in liquid nitrogen and stored at −80°C and were partly embedded in paraffin after fixation in 10% formalin for histologic diagnosis. All available H&E-stained slides were reviewed. The tumor grading was based on the criteria proposed by Edmondson and Steiner (I, well differentiated; II, moderately differentiated; III, poorly differentiated; and IV, undifferentiated; ref. 16). The conventional tumor-node-metastasis system outlined in Cancer Staging Manual (6th edition) published by the American Joint Committee on Cancer was used in tumor staging. The tumor size was obtained from the pathology reports.

RNA extraction and cDNA synthesis

RNA extraction and cDNA synthesis were carried out as described previously (17, 18). Briefly, total RNA was extracted from cancerous and surrounding noncancerous frozen tissues using an RNeasy minikit (Qiagen). The integrity of all tested total RNA samples was verified using a Bioanalyzer 2100 (Agilent Technologies). DNase I treatment was routinely included in the extraction step. Samples containing 4 μg of total RNA were incubated with 2 μL of 10 μmol/L oligo $d(T)_{18}$ primer (Genotech) at 70°C for 7 minutes and cooled on ice for 5 minutes. After adding the enzyme mix to the annealed total RNA sample, the reaction was incubated for 90 minutes at 42°C prior to heat inactivation of reverse transcriptase at 80°C for 10 minutes. The cDNA samples were brought up to a final volume of 400 μL by addition of diethylpyrocarbonate-treated water.

Quantitative real-time PCR

Real-time PCR amplifications were done as described previously (17, 18). Briefly, using ABI PRISM 7900HT instruments (Applied Biosystems), real-time PCR analysis was done in a total volume of 10 μL with the following amplification steps: an initial denaturation step at 95°C for 10 minutes, which was followed by 45 cycles of denaturation at 95°C for 15 seconds and elongation at 60°C for 1 minute. The primer and probe sequences were designed using Primer Express 3.0 software (Applied Biosystems), and all probe sequences were labeled with FAM at the 5′ end and with TAMRA at the 3′ end (Supplementary Table S1). The mRNA levels of *HMGB2* were measured (the threshold cycle, C_T) in triplicate and then normalized relative to a set of reference genes (*B2M*, *GAPDH*, *HMBS*, *HPRT1*, and *SDHA*) by subtracting the average of the mRNA levels of the five reference genes as an internal control (19). Using the ΔC_T values (*HMGB2* C_T − average C_T of reference genes), the mRNA copy number ratio was

Published OnlineFirst September 17, 2010; DOI: 10.1158/1078-0432.CCR-10-0825

Table 1. Relations between HMGB2 mRNA and protein levels and clinicopathologic features in HCC

Clinicopathologic parameters	RT-PCR (n = 334)			Immunohistochemistry (n = 173)		
	High HMGB2 (n = 130)	Low HMGB2 (n = 204)	P	High HMGB2 (n = 64)	Low HMGB2 (n = 109)	P
Age			0.81			0.42
<55 y	86	131		28	56	
≥55 y	44	73		36	53	
Gender			0.24			0.12
Male	98	166		47	92	
Female	32	38		17	17	
HBV			0.033			0.66
Absent	19	51		16	32	
Present	111	153		48	77	
HCV			0.37			0.90
Absent	127	194		60	104	
Present	3	10		4	5	
Liver cirrhosis			0.052			0.65
Absent	57	113		31	58	
Present	73	91		33	51	
Tumor stage			0.21			0.12
I	39	80		22	53	
II	61	86		28	42	
III and IV	30	38		14	14	
AFP level			0.025			0.58
<100 ng/mL	60	121		37	69	
≥100 ng/mL	70	83		27	40	
Vascular invasion			0.14			0.14
Absent	41	82		23	53	
Present	89	122		41	56	
Tumor number			0.53			0.99
Single	104	156		52	90	
Multiple	26	48		12	19	
Tumor size			0.90			0.34
<5 cm	76	122		35	69	
≥5 cm	54	82		29	40	
Edmondson grade			0.025			0.97
I	4	23		5	9	
II	113	165		56	94	
III and IV	13	16		3	6	

NOTE: Cutoff value for *HMGB2* mRNA copy number ratio was 0.145, and cutoff value for HMGB2 histoscore was 30.
Abbrevations: AFP, α-fetoprotein; HBV, hepatitis B virus; HCV, hepatitis C virus.

calculated as $2^{-\Delta CT}$. Standard curves were constructed from the results of simultaneous amplifications of cDNA samples diluted serially.

Immunohistochemical analysis

Immunohistochemical staining was done on 4-μm-thick, formalin-fixed, paraffin-embedded tissue sections. Tissue sections were deparaffinized three times in xylene for a total of 15 minutes and subsequently rehydrated. Antigen retrieval was done by boiling in Tris-EDTA buffer (pH 9.0) using a microwave for 5 minutes twice. Slides were then incubated with antihuman HMGB2 mouse monoclonal antibody (M03), clone 3C7 (Abnova), for 1 hour at room temperature with an antibody dilution of 1:280. The antigen-antibody reaction was detected using the DAKO REAL Detection System (LSAB+) K5001 (DAKO). Counterstaining was done with Mayer's hematoxylin.

All the immunohistochemically stained sections were evaluated in a semiquantitative fashion by two pathologists as previously described (20). Nuclear staining was considered positive. To evaluate the expressions of HMGB2, 10 fields within the tumor showing nuclear

Published OnlineFirst September 17, 2010; DOI: 10.1158/1078-0432.CCR-10-0825

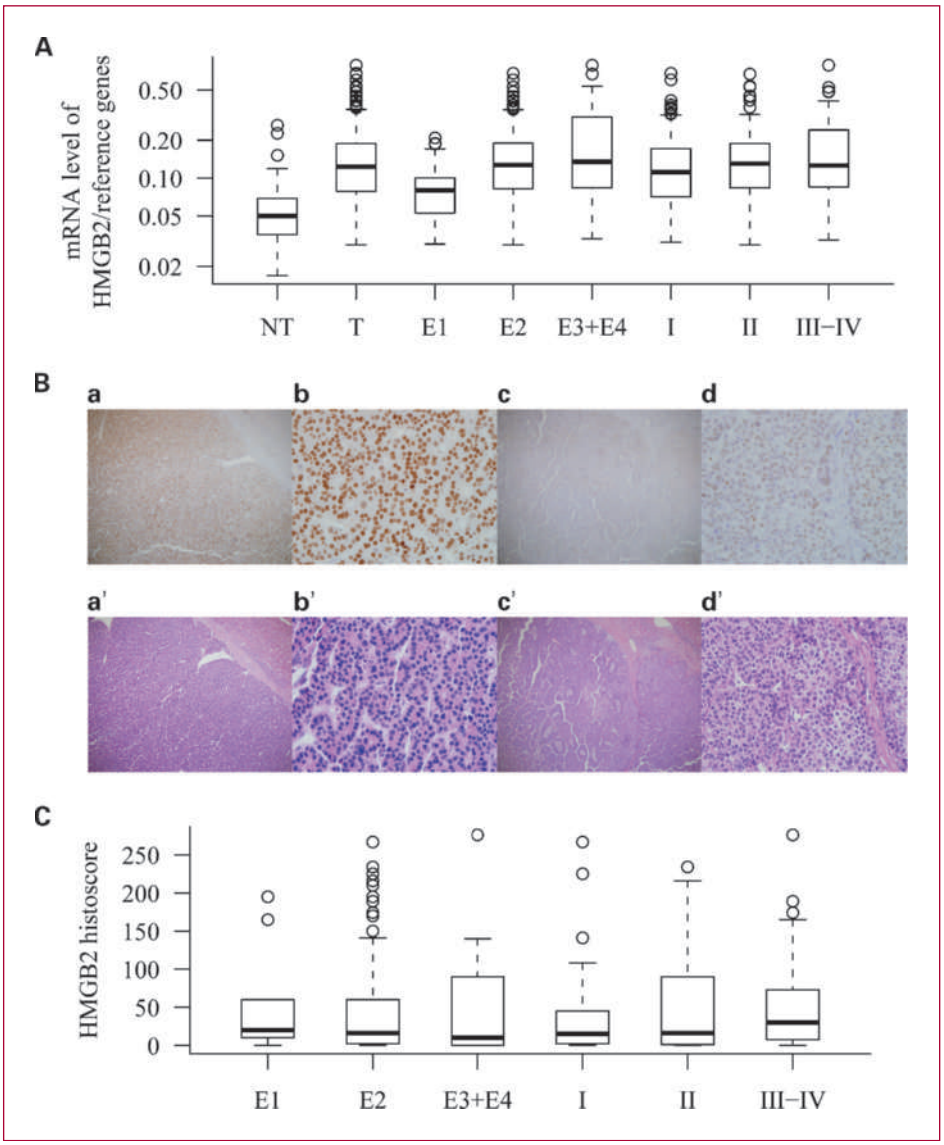

Fig. 1. RT-PCR and immunohistochemistry of HMGB2 in HCC. A, box and whisker plot for *HMGB2* mRNA levels as determined by real-time RT-PCR. The box is marked by the first and third quartile with the median marked by a thick line. The whiskers extend to the most extreme data point, which is no more than 1.5 times the interquartile range from the box. B, representative strong (a, b) and weak (c, d) HMGB2-positive samples at 40× (a, c) and 400× (b, d) magnification. Background livers, included in top right corners of a and c, showed negative HMGB2 staining. The corresponding H&E staining are shown in a' to d'. C, box and whisker plot for HMGB2 expression levels determined by immunohistochemistry. NT, noncancerous liver; T, all HCC; E1, Edmondson grade I; E2, Edmondson grade II; E3 + E4, Edmondson grade III or IV; I, stage I; II, stage II; III-IV, stage III or IV.

staining in low-power view (40×) were selected, and the HMGB2 expression was evaluated in 10 high-power fields (400×). Intensities were classified as 0 (no staining), 1 (weak staining), 2 (moderate staining), and 3 (strong staining). For each stained section, a value-designated histochemical score (histoscore) was obtained as follows: histoscore = $\Sigma(i \times Pi)$, where i and Pi represent the intensity and percentage of cells that were stained at each intensity, respectively.

Cell culture

Human HCC cell lines SK-Hep-1, SH-J1, and Hep3B were used in this study. SK-Hep-1 and Hep3B were obtained from the American Type Culture Collection, and SH-J1 was kindly provided by Dr. Dae-Ghon Kim of the Chonbuk National University Medical School (21). All cells were cultured in DMEM supplemented with 10% fetal bovine serum at 37°C under 5% CO_2. For the setting of cell death, cells were treated with 30 μmol/L cisplatin (Sigma-Aldrich), or 20 μmol/L etoposide (Sigma-Aldrich) for 36 hours.

Gene silencing and overexpression

For small interfering RNA (siRNA) transfection, the 19-nucleotide siRNA duplexes (5′-CUGAACAUCGCCCAAAGAU-3′) with a 3′-dTdT overhang, targeting the *HMGB2* gene or the negative control duplex (5′-CCUACGCCACCAAUUUC-GU-3′), were synthesized (Bioneer). *HMGB2*-expressing plasmid (HMGB2-pcDNA3.1+) has been previously described (22). These siRNA duplexes (100 nmol/L) and plasmid DNA (10 μg) were introduced into SK-Hep-1, SH-J1, and Hep3B cells cultured in 24-well plates for

Published OnlineFirst September 17, 2010; DOI: 10.1158/1078-0432.CCR-10-0825

72 hours or as indicated in Fig. 3 using Lipofectamine 2000 (Invitrogen) according to the manufacturer's instructions.

Cell viability assay and fluorescence-activated cell sorting analysis

To determine cell viability, a cell proliferation assay kit (CellTiter 96 AQ_{ueous} One Solution; Promega) containing the MTS reagent was used according to the manufacturer's protocols. The change of absorbance at 492 nm was monitored using a microplate reader (Spectrafluor Plus; Tecan). To assess apoptotic cell death, flow cytometric analysis was done (FACSCalibur; BD Biosciences). Cells were fixed with ethanol at −20°C for 1 hour, washed with cold PBS three times, and then incubated with propidium iodide and RNase A at room temperature in the dark for 30 minutes. Apoptotic cells were estimated with sub-G_1 fraction of cells gated to distinguish singlet from aggregated cells. These results were analyzed with CellQuestPro software.

Western blot analysis

Cells were lysed in the radioimmunoprecipitation assay buffer on ice for 15 minutes. The whole-cell lysates were clarified by centrifugation at 15,000 × *g* for 15 minutes at 4°C, and the protein concentration in the supernatant was determined by the Bradford method. Equal amounts of lysates were resolved on SDS-PAGE. Proteins on gels were then transferred to NC membrane (Whatman). The transferred membranes were blocked with 4% skim milk for 1 hour and incubated with primary antibodies for 2 hours at room temperature. After incubation with horseradish peroxidase–conjugated secondary antibodies (Zymed) for 1 hour at room temperature, the immunoblots were visualized by SuperSignal West Pico Luminol/Enhancer solution (Thermo Fisher Scientific). Polyclonal rabbit antibodies against human HMGB2 (Abcam) and anti-actin polyclonal goat antibodies (Santa Cruz Biotechnology) were used for immunoblot analyses. The intensity of each protein band was analyzed using NIH Image J program.

Statistical analysis

All statistical analyses were done with the open source statistical programming environment R. Significant differences between gene and protein expression levels were evaluated by a Student's *t* test. Spearman's correlation coefficient was calculated to show the correlation in the expression of HMGB2 mRNA and protein. Receiver operating characteristic (ROC) curves for death within 5 years were used to find cutoff values of HMGB2 mRNA level and histoscores. Correlation between gene expression and clinicopathologic variables was evaluated using a χ^2 test. Kaplan-Meier survival curves were calculated using tumor recurrence (defined as the first appearance of a tumor at any site following definitive treatment) or death as the end points. The difference of the overall survival (OS) curve, disease-free survival (DFS) curve, or time-to-recurrence curve was examined by log-rank test. In addition, the Cox proportional hazard regression model was used to identify independent prognostic factors for OS. A two-tailed *P* value test was used with a *P* value of <0.05 considered statistically significant.

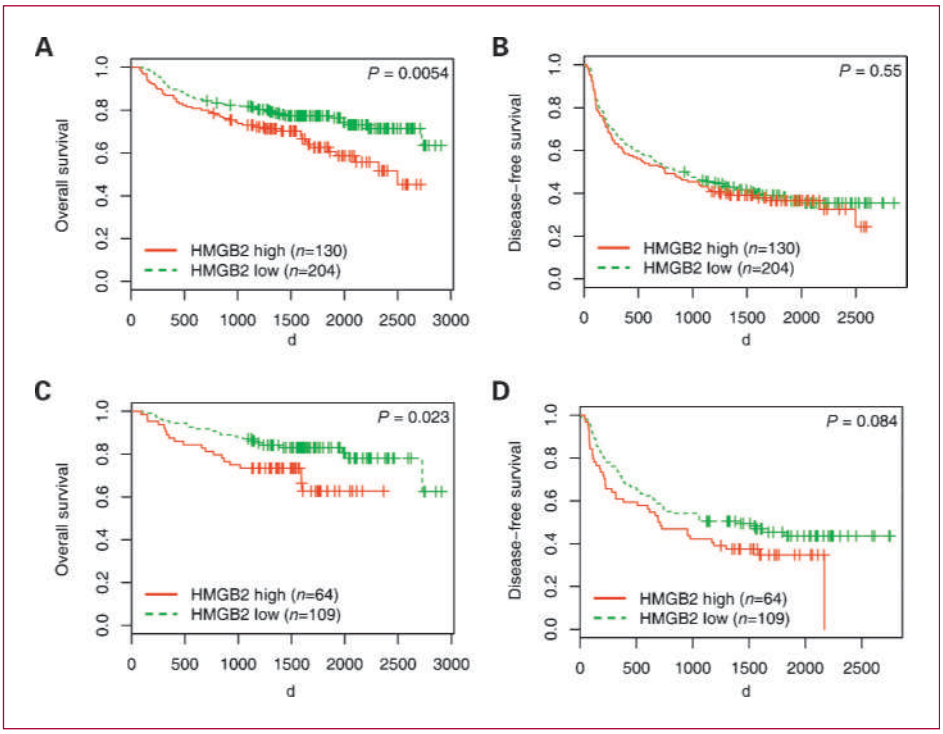

Fig. 2. Kaplan-Meier curves for OS and DFS of patients with high and low HMGB2 expression levels after surgery. A and B, patients with high *HMGB2* mRNA levels (≥0.145; copy number ratio) had a significantly shorter OS time (*P* = 0.0054). However, no significant difference in DFS time was observed (*P* = 0.55). Broken lines, patients with low *HMGB2* mRNA levels (*n* = 204); thin lines, patients with high *HMGB2* mRNA levels (*n* = 130). C and D, patients with high HMGB2 histoscores (≥30) had a significantly shorter OS time (*P* = 0.023) and tended to have a shorter DFS time (*P* = 0.084). Broken lines, patients with low HMGB2 histoscores (*n* = 109); thin lines, patients with high HMGB2 histoscores (*n* = 64).

Published OnlineFirst September 17, 2010; DOI: 10.1158/1078-0432.CCR-10-0825

Results

Overexpression of HMGB2 in HCC

We did real-time RT-PCR for *HMGB2* mRNA from frozen paired samples derived from 334 patients with HCC. A total of 334 HCCs and 109 noncancerous hepatic samples were assessed by real-time RT-PCR. Expression of *HMGB2* mRNA was measured in triplicate and was then normalized relative to the expression of a set of reference genes (*B2M*, *GAPDH*, *HMBS*, *HPRT1*, and *SDHA*) as an internal control (19). *HMGB2* mRNA was significantly higher in HCC than in noncancerous hepatic tissues (0.154 versus 0.057; mean

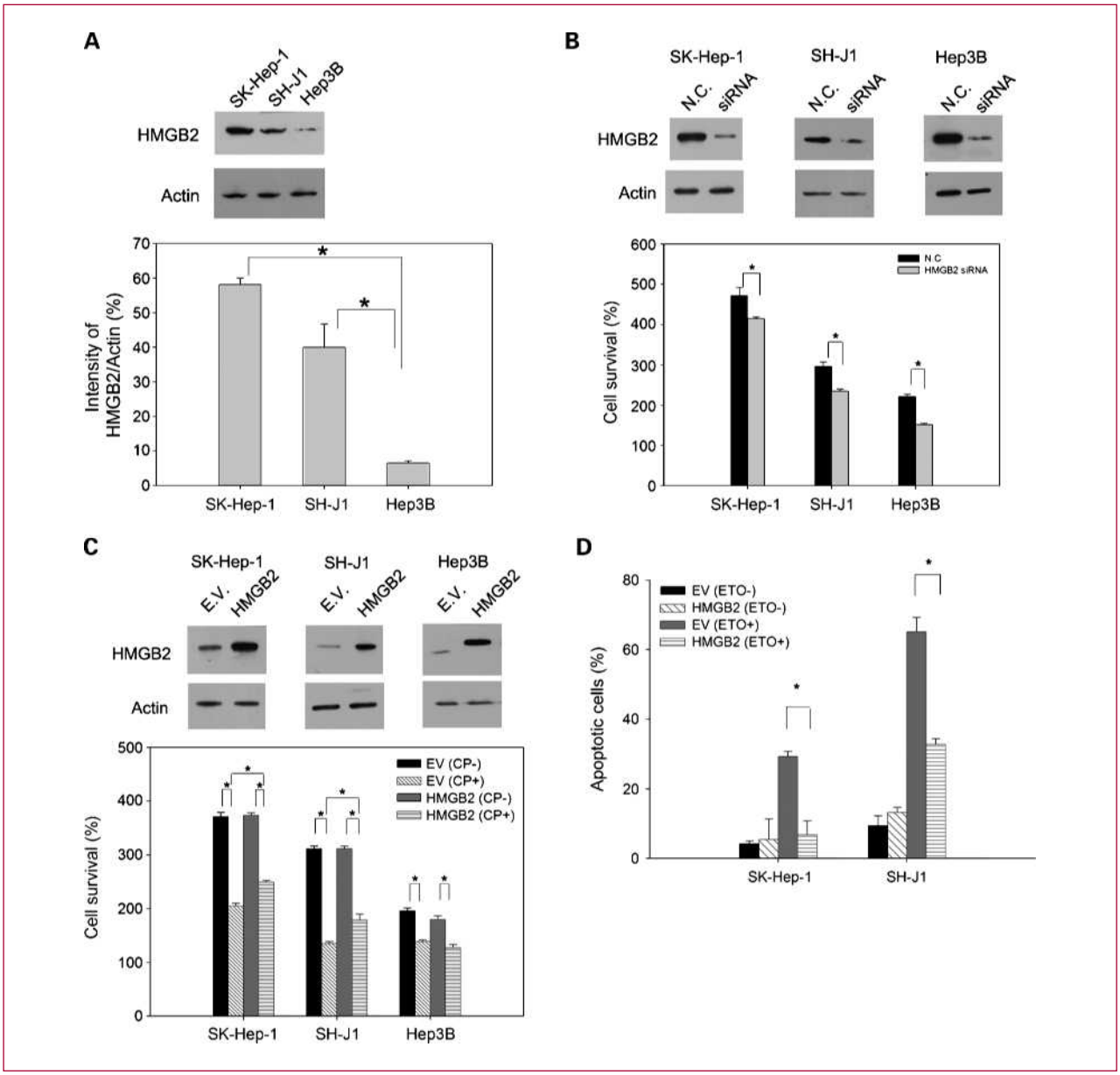

Fig. 3. Effects of HMGB2 levels on cell survival in the *HMGB2* knockdown and *HMGB2* transfection experiments. A, expression of HMGB2 in three HCC cell lines was detected by immunoblot using β-actin as a loading control. B, *HMGB2* siRNA-transfected cells showed efficient silencing as shown by immunoblot analysis 48 h after transfection. Significant reduction of cell viability by *HMGB2* knockdown was confirmed by MTS assay 72 h after transfection. C, cells were cultured for 36 h in the absence or presence of 30 μmol/L cisplatin 24 h after transfection (CP-, no cisplatin treatment; CP+, cisplatin treatment). All cells showed significant reduction of viability on cisplatin treatment, but overexpression of *HMGB2* increased cisplatin resistance in SK-Hep-1 and SH-J1 cells. For histograms in B and C, the final cell survival (%) values were calculated relative to the value at the time of transfection, which was set to be 100%. D, cells were cultured for 36 h in the absence or presence of 20 μmol/L etoposide 24 h after transfection (ETO-, no etoposide treatment; ETO+, etoposide treatment). The sub-G_1 DNA contents were measured as an apoptotic fraction. Data shown are mean values ± SD of three independent experiments (*, $P < 0.05$). NC, negative control siRNA; EV, empty vector; CP, cisplatin; ETO, etoposide.

Published OnlineFirst September 17, 2010; DOI: 10.1158/1078-0432.CCR-10-0825

Table 2. Univariate Cox regression analysis for OS

Variable	OS RT-PCR (n = 334)		OS immunohistochemistry (n = 173)	
	HR (95% CI)	P	HR (95% CI)	P
Age (<55 y versus ≥55 y)	0.76 (0.49–1.16)	0.20	1.18 (0.64–2.19)	0.60
Gender (male versus female)	0.82 (0.50–1.35)	0.43	0.99 (0.45–2.13)	0.97
Edmondson grade (I-II versus III-IV)	1.98 (1.12–3.48)	0.018	2.27 (0.81–6.37)	0.12
HBV (absent versus present)	1.68 (0.97–2.91)	0.064	1.41 (0.67–2.96)	0.36
HCV (absent versus present)	1.47 (0.60–3.63)	0.40	1.67 (0.51–5.41)	0.40
AFP level (<100 ng/mL versus ≥100 ng/mL)	2.46 (1.64–3.71)	1.6×10^{-5}	1.43 (0.77–2.64)	0.25
Liver cirrhosis (absent versus present)	1.35 (0.91–2.00)	0.14	1.14 (0.62–2.11)	0.67
Vascular invasion (absent versus present)	6.59 (3.42–12.7)	1.6×10^{-8}	5.65 (2.37–13.5)	9.2×10^{-5}
Tumor number (single versus multiple)	4.29 (2.89–6.38)	$<1 \times 10^{-12}$	3.90 (2.05–7.42)	3.5×10^{-5}
Tumor size (<5 cm versus ≥5 cm)	3.53 (2.33–5.34)	2.5×10^{-9}	2.65 (1.41–4.96)	0.0024
Tumor stage (I-II versus III-IV)	7.02 (4.71–10.5)	$<1 \times 10^{-12}$	7.68 (4.08–14.4)	2.4×10^{-10}
HMGB2 (low versus high)	1.74 (1.17–2.58)	0.006	2.04 (1.09–3.81)	0.026

Abbreviations: HR, hazard ratio; CI, confidence interval.

copy number ratio, $P < 0.0001$; Fig. 1A). *HMGB2* mRNA levels significantly increased according to tumor differentiation (Edmondson grade I versus II, I versus III and IV, $P < 0.01$; Edmondson grade II versus III and IV, $P = 0.059$). On the other hand, the average *HMGB2* mRNA levels increased according to clinical stage (I < II < III and IV), but the differences were not statistically significant (Fig. 1A). The average *HMGB2* mRNA level was higher for tumors with vascular invasion, but the difference was not statistically significant (0.14 versus 0.16, $P = 0.11$). No difference was found in *HMGB2* mRNA level after categorization by tumor size or tumor number (Supplementary Fig. S1A–C). HMGB2 protein expression was evaluated by immunohistochemistry on 173 HCC specimens (157 randomly selected samples from tumors analyzed by RT-PCR and 16 additional independent cases). Immunostaining revealed that HMGB2 was expressed much higher in HCC than in noncancerous hepatic tissues, which was observed primarily in the nucleus (Fig. 1B). The average HMGB2 histoscores increased according to tumor differentiation (Edmondson grade I < II < III and IV) and clinical stage (I < II < III and IV), but the differences were not statistically significant (Fig. 1C). The HMGB2 histoscore was significantly higher for tumors with vascular invasion ($P = 0.045$) and tended to be higher for large tumors ($P = 0.063$), but no difference was found in HMGB2 histoscore by tumor number (Supplementary Fig. S1D–F). There was a significant positive correlation between HMGB2 mRNA level and histoscore ($\rho = 0.35$, $P < 0.001$; data not shown).

Correlation between mRNA and protein levels of HMGB2 and clinicopathologic features

For a better understanding of the significance of HMGB2 expression in HCC, mRNA and protein expression levels were correlated with the major clinicopathologic features. The cutoff values of HMGB2 mRNA and protein levels were determined as the points that discriminate between patients with good prognosis and poor prognosis from the ROC curves for death within 5 years (Supplementary Fig. S2). As shown in Table 1, high *HMGB2* mRNA expression was correlated with HBV infection ($P = 0.033$), high α-fetoprotein (AFP) level ($P = 0.025$), and Edmondson grade ($P = 0.025$). However, no correlation was observed between the HMGB2 histoscore and clinicopathologic parameters by a χ^2 test (Table 1).

Effect of tumor HMGB2 mRNA and protein levels on prognosis

During the follow-up observation period of up to 95.6 months, locoregional recurrence or distant metastases occurred in 208 patients (59.4%) and death was confirmed in 104 patients (29.7%). To assess the prognostic significance of HMGB2 expression, ROC curve for death within 5 years was constructed (Supplementary Fig. S2). The area under the curve of the ROC curve of *HMGB2* mRNA level was 0.594 ($P = 0.006$), and the area under the curve of the ROC curve of HMGB2 histoscore was 0.594 ($P = 0.038$). The cutoff values of HMGB2 mRNA level ($\theta = 0.145$; 53.7% sensitivity, 65.1% specificity, and 62.1% accuracy) and HMGB2 histoscore ($\theta = 30$; 50.0% sensitivity, 66.7% specificity, and 63.0% accuracy) were chosen based on accuracy. The prognostic significance of HMGB2 expression was further analyzed using the Kaplan-Meier method. At the 5- and 7-year follow-up, 78% and 72% of the patients with low *HMGB2* expression (<0.145; copy number ratio) survived, whereas 64% and 46% of the patients with high *HMGB2* expression (≥0.145; copy number ratio) survived, respectively (Fig. 2A). The log-rank test showed that patients with

Published OnlineFirst September 17, 2010; DOI: 10.1158/1078-0432.CCR-10-0825

Table 3. Multivariate Cox regression analysis for OS

Variable	OS RT-PCR (n = 334)		OS immunohistochemistry (n = 173)	
	HR (95% CI)	P	HR (95% CI)	P
HMGB2 (low versus high)	1.86 (1.22–2.83)	0.0037	1.67 (0.88–3.17)	0.11
Age (<55 y versus ≥55 y)	1.03 (0.66–1.61)	0.90	1.24 (0.66–2.32)	0.51
Edmondson grade (I-II versus III-IV)	1.23 (0.69–2.20)	0.48		
AFP level (<100 ng/mL versus ≥100 ng/mL)	1.14 (0.73–1.80)	0.56		
Vascular invasion (absent versus present)	3.11 (1.53–6.30)	0.0017	2.97 (1.14–7.76)	0.026
Tumor number (single versus multiple)	1.39 (0.78–2.51)	0.27	1.17 (0.51–2.69)	0.72
Tumor size (<5 cm versus ≥5 cm)	1.89 (1.19–3.01)	0.0073	1.32 (0.66–2.63)	0.43
Tumor stage (I-II versus III-IV)	2.91 (1.58–5.38)	0.0006	3.95 (1.68–9.26)	0.0016

Abbreviations: HR, hazard ratio; CI, confidence interval.

high *HMGB2* mRNA levels had a significantly shorter OS time (P = 0.0054). However, no significant difference in DFS time (Fig. 2B) or time to recurrence (Supplementary Fig. S3A) was observed. Similarly, patients with high HMGB2 histoscores (≥30) had a significantly shorter OS time (P = 0.023; Fig. 2C) and tended to have a shorter DFS time (P = 0.084; Fig. 2D). However, no significant difference in time to recurrence was observed (Supplementary Fig. S3B).

Furthermore, subgroup analysis indicated that significant differences in OS time were found between groups with high and low *HMGB2* mRNA levels after categorization by the following variables: single tumor (P = 0.00046), moderately differentiated tumor (P = 0.020), tumor stage I (P = 0.040), low AFP level (P = 0.00041), and large tumor (P = 0.0057, log-rank test; Supplementary Fig. S4). Significant differences in OS time were found between high and low HMGB2 histoscore groups after categorization by the following variables: single tumor (P = 0.029), low AFP level (P = 0.020), and small tumor (P = 0.034, log-rank test; Supplementary Fig. S5).

A univariate Cox regression analysis was used to identify important prognostic factors of OS. For the 334-patient cohort analyzed by RT-PCR, a high *HMGB2* mRNA level (P = 0.006), high Edmondson grade (P = 0.018), high AFP level ($P = 1.6 \times 10^{-5}$), large tumor size ($P = 2.5 \times 10^{-9}$), vascular invasion ($P = 1.6 \times 10^{-8}$), tumor multiplicity ($P < 1 \times 10^{-12}$), and high tumor stage ($P < 1 \times 10^{-12}$) were identified as important risk factors for OS. For the 173-patient cohort analyzed by immunohistochemistry, a high HMGB2 protein level (P = 0.026), large tumor size (P = 0.0024), vascular invasion ($P = 9.2 \times 10^{-5}$), tumor multiplicity ($P = 3.5 \times 10^{-5}$), and high tumor stage ($P = 2.4 \times 10^{-10}$) were identified as important risk factors for OS (Table 2). Because the cohort analyzed by immunohistochemistry had more patients older than 55 years compared with the cohort analyzed by RT-PCR (Supplementary Table S2), the multivariate Cox model included age as well as all the important risk factors from univariate analysis. In a multivariate Cox analysis, high *HMGB2* mRNA expression (P = 0.0037), vascular invasion (P = 0.0017), large tumor size (P = 0.0073), and high tumor stage (P = 0.0006) were found to be independent poor prognostic factors for OS in the patient cohort analyzed by RT-PCR. However, vascular invasion (P = 0.026) and high tumor stage (P = 0.0016) were found to be independent poor prognostic factors for OS in the patient cohort analyzed by immunohistochemistry (Table 3). Because tumor stage uses information from other variables (vascular invasion, tumor size, and tumor number), we also analyzed a multivariate Cox model without tumor stage (Supplementary Table S3). *HMGB2* mRNA expression remained an independent prognostic factor (P = 0.0035); however, HMGB2 histoscore was still not an independent prognostic factor (P = 0.068). When the subgroup of 157 patients included in both RT-PCR and immunohistochemistry cohorts were analyzed by multivariate Cox model, both *HMGB2* mRNA expression (P = 0.035) and HMGB2 histoscore (P = 0.043) were independent prognostic factors after controlling for vascular invasion, tumor number, and tumor size (Supplementary Table S4).

Expression of HMGB2 in HCC cell lines

We selected three HCC cell lines, SK-Hep-1, SH-J1, and Hep3B, to investigate their HMGB2 expression levels as determined by Western blot analysis. High expression of HMGB2 was observed in SK-Hep-1 and SH-J1, whereas Hep3B showed the lowest level of HMGB2 protein (Fig. 3A).

Effect of HMGB2 knockdown on cell viability

We investigated whether modulating the HMGB2 level could affect cell viability. Toward this end, these HCC cells were subjected to the gene knockdown studies. Cell survivals were determined by MTS assay following the transfection of siRNA targeting *HMGB2*. Each HCC cell line transfected with *HMGB2* siRNA showed efficient silencing

Published OnlineFirst September 17, 2010; DOI: 10.1158/1078-0432.CCR-10-0825

of *HMGB2* expression, as judged by immunoblot analysis (Fig. 3B). In cell viability assay, all HCC cell lines showed significant reduction of cell viability by *HMGB2* knockdown compared with negative control group (Fig. 3B), suggesting that HMGB2 contributes to the survival of HCC cells.

Effect of HMGB2 overexpression on cisplatin- and etoposide-induced cell death

To further characterize the function of HMGB2 in HCC cell survival, we investigated the effects of HMGB2 overexpression. *HMGB2* overexpression had no significant effect on cell viability under normal culture conditions (Fig. 3C). These observations raised the possibility that HMGB2 might affect the antiapoptotic pathway in HCC. Therefore, cell death was induced in all HCC cells by treatment with cisplatin, a well-known inducer of apoptosis, concomitant with the overexpression of *HMGB2*. As shown in Fig. 3C, SK-Hep-1 and SH-J1 cells were more resistant to the cisplatin-induced cell death when *HMGB2* was overexpressed. However, Hep3B did not show a significant difference in cell viability. To further explore the role of HMGB2 on chemotherapeutic drug treatment, etoposide was used to induce apoptosis in these cell lines. In the presence of etoposide, the percentage of apoptotic cells (sub-G_1 fraction) were 36.0 ± 1.4% in SK-Hep-1 transfected with empty vector, whereas only 8.2 ± 3.9% of SK-Hep-1 cells transfected with *HMGB2* were apoptotic as quantified by flow cytometry (Fig. 3D). SH-J1 also showed lower sub-G_1 fraction (32.75 ± 1.6%) when *HMGB2* was overexpressed compared with cells transfected with empty vector (65.15 ± 4.1%). These results suggest that HMGB2 inhibits cell apoptosis in some HCC cell lines.

Discussion

The present study highlighted HMGB2, a ubiquitous nuclear regulator of chromatin, as a signature molecule correlated with the survival of HCC cells *in vitro* as well as the prognosis of HCC patients. To our knowledge, we present the first large-scale study using real-time RT-PCR and immunohistochemistry analyses to examine the prognostic effect of HMGB2 expression in HCC for a randomly selected population of HCC patients.

It was found that HCC patients with HMGB2 overexpression were at significantly high risk of short OS. Multivariate Cox analysis further indicated that the mRNA level of *HMGB2* was an independent prognostic factor along with the well-established factors including tumor vascular invasion, tumor size, and tumor stage. In the current study, although HMGB2 protein level was correlated with the survival of patients, it was not significant in a multivariate analysis. On the other hand, when only the 157 patients included in both RT-PCR and immunohistochemistry cohorts were analyzed by multivariate Cox model, both HMGB2 mRNA level and histoscore were independent prognostic factors after controlling for vascular invasion, tumor number, and tumor size, indicating that the different prognostic significance of HMGB2 mRNA and protein level could be due to differences in patient cohorts of this study. Subgroup analysis further indicated that HMGB2 expression was correlated with OS of patients after categorization by several clinicopathologic variables. Both HMGB2 mRNA level and histoscores were correlated with OS of patients with single tumor and patients with low serum AFP level. Taken together, our present data suggest that HMGB2 expression is a significant prognostic factor and might play an important role in the progression of HCC.

This prompted us to examine the biological function of HMGB2 in greater detail through *in vitro* analysis of HCC cell lines. Downregulation of *HMGB2* expression by siRNA could significantly reduce the proliferation of HCC cell lines. These observations support our conclusions from our clinical data that HMGB2 overexpression is correlated with poor prognosis in HCC. Consistent with our results, *HMGB2* inhibition by antisense RNA repressed cell cycle progression in COS-1 cells (23) and *HMGB2* knockdown by siRNA inhibited cell proliferation in rat HCC cells (15).

With respect to DNA binding proteins, HMGB1 and HMGB2 are closely related to the susceptibility of cells to DNA damage–induced cell death. Platinum therapy characteristically creates DNA adducts reparable by an excision repair system. HMG domain motifs bind specifically to the major platinum DNA dGpG adducts, creating a shield against human excision nucleases, signifying its potential role in affecting sensitivity and resistance of cancer cells (24, 25). We showed that a transient expression of HMGB2 conferred resistance to cisplatin-induced cell death in HCC cell lines, SK-Hep-1 and SH-J1. In addition, these cell lines elicited significantly less apoptosis in response to another chemotherapeutic drug, etoposide, on overexpression of *HMGB2*. This suggested that HMGB2 could diminish apoptotic cell death through cisplatin-independent mechanism as judged by etoposide treatment. These results indicate that HMGB2 may exert a role as an antiapoptotic oncoprotein in HCC. On the other hand, the introduction of *HMGB2* gene into human lung cancer cells increased cisplatin sensitivity (26), indicating that the role of HMGB2 might be dependent on types of cancer. HMGB2 suppressed the transcriptional activity of p53 in osteosarcoma (27), whereas HMGB2 enhanced the transcriptional activity of p53 in E6-positive cervical cancer, HeLa (22). Because HMGB2 is a DNA-binding protein, HMGB2 may interact with a number of proteins, including transcription factors, cofactors, and repressors, and thereby possibly act in a tissue-specific manner. In agreement with our results, HMGB1 has been shown to be upregulated in cisplatin-resistant cancer cells (10). Beyond the involvement of HMGB proteins in the cisplatin-associated cell susceptibility, HMGBs are also of importance in the antiapoptotic pathway. HMGB1 was shown to activate NF-κB to induce an antiapoptotic gene, *c-IAP2*, thereby promoting cell viability in apoptosis-triggering conditions (28). Taken together, HMGB2 could be of particular relevance to apoptosis pathway in HCC.

Published OnlineFirst September 17, 2010; DOI: 10.1158/1078-0432.CCR-10-0825

Because HMGB2 is highly homologous to HMGB1, it may have similar effects with regard to neoplastic development. Overexpression of HMGB1 has been observed in several cancers including HCC (29, 30). Furthermore, HMGB1 has been shown to stimulate the migration of smooth muscle cells and fibroblasts, whereas anti-HMGB1 antibodies inhibited the migration of neuroblastoma and glioma cells (31, 32). HCC tissues have been shown to overexpress receptors for advanced glycation end products that could relay HMGB signals (33), indicating a potentially important function of HMGBs (34). HMGB2 has been reported to interact with steroid receptors (35), p53 and p73 (27). In addition, HMGB2 has been reported to be significantly downregulated by anti-human epidermal growth factor receptor 2 antibody through the AKT pathway in breast cancer cell lines (36). Recently, HMGB2 was shown to potentiate Wnt/β-catenin signaling in articulate cartilage (37). These possible functional links of HMGB2 to other important cellular regulators in the context of HCC development and progression warrant further investigation.

In conclusion, we found that HMGB2 expression could be associated with HCC progression and that *HMGB2* mRNA level was an independent prognostic factor for OS in HCC patients. The possible role of HMGB2 in the antiapoptotic pathway highlights the importance of HMGB2 as a potential diagnostic and therapeutic target of HCC. Therefore, HMGB proteins merit further study with respect to the molecular pathogenesis and control of HCC.

Disclosure of Potential Conflicts of Interest

No potential conflicts of interest were disclosed.

Grant Support

CbsBioscience intramural research funds CBS-08-71 (J.Y. Park) and the Human Resource Training Project for Regional Innovation through the Ministry of Education, Science and Technology and Korea Institute for Advancement of Technology and the 21C Frontier Functional Human Genome Project, Ministry of Science and Technology of Korea grant FG-06-11-05 (K.Y. Choi).

The costs of publication of this article were defrayed in part by the payment of page charges. This article must therefore be hereby marked *advertisement* in accordance with 18 U.S.C. Section 1734 solely to indicate this fact.

Received 03/31/2010; revised 08/14/2010; accepted 09/08/2010; published OnlineFirst 09/17/2010.

References

1. Llovet JM, Burroughs A, Bruix J. Hepatocellular carcinoma. Lancet 2003;362:1907–17.
2. Parkin DM, Bray F, Ferlay J, Pisani P. Global cancer statistics, 2002. CA Cancer J Clin 2005;55:74–108.
3. Bosch FX, Ribes J, Diaz M, Cleries R. Primary liver cancer: worldwide incidence and trends. Gastroenterology 2004;127:S5–16.
4. Thorgeirsson SS, Grisham JW. Molecular pathogenesis of human hepatocellular carcinoma. Nat Genet 2002;31:339–46.
5. Thomas JO. HMG1 and 2: architectural DNA-binding proteins. Biochem Soc Trans 2001;29:395–401.
6. Pallier C, Scaffidi P, Chopineau-Proust S, et al. Association of chromatin proteins high mobility group box (HMGB) 1 and HMGB2 with mitotic chromosomes. Mol Biol Cell 2003;14:3414–26.
7. Hock R, Furusawa T, Ueda T, Bustin M. HMG chromosomal proteins in development and disease. Trends Cell Biol 2007;17:72–9.
8. Lotze MT, Tracey KJ. High-mobility group box 1 protein (HMGB1): nuclear weapon in the immune arsenal. Nat Rev Immunol 2005;5:331–42.
9. Pardo M, García Á, Thomas B, et al. The characterization of the invasion phenotype of uveal melanoma tumour cells shows the presence of MUC18 and HMG-1 metastasis markers and leads to the identification of DJ-1 as a potential serum biomarker. Int J Cancer 2006;119:1014–22.
10. Nagatani G, Nomoto M, Takano H, et al. Transcriptional activation of the human HMG1 gene in cisplatin-resistant human cancer cells. Cancer Res 2001;61:1592–7.
11. Balasubramani M, Day BW, Schoen RE, Getzenberg RH. Altered expression and localization of creatine kinase B, heterogeneous nuclear ribonucleoprotein F, high mobility group box 1 protein in the nuclear matrix associated with colon cancer. Cancer Res 2006; 66:763–9.
12. He Q, Liang CH, Lippard SJ. Steroid hormones induce HMG1 overexpression and sensitize breast cancer cells to cisplatin and carboplatin. Proc Natl Acad Sci U S A 2000;97:5768–72.
13. Pasheva EA, Pashev IG, Favre A. Preferential binding of high mobility group 1 protein to UV-damaged DNA. Role of the COOH-terminal domain. J Biol Chem 1998;273:24730–6.
14. Huang J-C, Zamble DB, Reardon JT, Lippard SJ, Sancar A. HMG-domain proteins specifically inhibit the repair of the major DNA adduct of the anticancer drug cisplatin by human excision nuclease. Proc Natl Acad Sci U S A 1994;91:10394–8.
15. Suzuki S, Takeshita K, Asamoto M, et al. High mobility group box associated with cell proliferation appears to play an important role in hepatocellular carcinogenesis in rats and humans. Toxicology 2009;255:160–70.
16. Edmondson H, Steiner P. Primary carcinoma of the liver: a study of 100 cases among 48,900 necropsies. Cancer 1954;7:462–503.
17. Kim J, Hong SJ, Park JH, et al. Real-time reverse transcription PCR analysis for validation of transketolase gene in hepatocellular carcinoma tissues. Biochip J 2009;3:130–8.
18. Kim J, Hong SJ, Lim EK, et al. Expression of nicotinamide N-methyltransferase in hepatocellular carcinoma is associated with poor prognosis. J Exp Clin Cancer Res 2009;28:20.
19. Vandesompele J, Preter KD, Pattyn F, et al. Accurate normalization of real-time quantitative RT-PCR data by geometric averaging of multiple internal control genes. Genome Biol 2002;3: RESEARCH0034.
20. Alam SM, Fujimoto J, Jahan I, Sato E, Tamaya T. Coexpression of EphB4 and ephrinB2 in tumour advancement of ovarian cancers. Br J Cancer 2008;98:845–51.
21. Kim D-G, Park S-Y, Kim H, Chun Y-H, Moon W-S, Park S-H. A comprehensive karyotypic analysis on a newly established sarcomatoid hepatocellular carcinoma cell line SH-J1 by comparative genomic hybridization and chromosome painting. Cancer Genet Cytogenet 2002;132:120–4.
22. Lee D, Kwon J-H, Kim EH, Kim E-S, Choi KY. HMGB2 stabilizes p53 by interfering with E6/E6AP-mediated p53 degradation in human papillomavirus-postive HeLa cells. Cancer Lett 2010;292: 125–32.
23. Yamazaki F, Nagatsuka Y, Shirakawa H, Yoshida M. Repression of cell cycle progression by antisense HMG2 RNA. Biochem Biophys Res Commun 1995;210:1045–51.
24. Mitkova E, Ugrinova I, Pashev IG, Pasheva EA. The inhibitory effect

Published OnlineFirst September 17, 2010; DOI: 10.1158/1078-0432.CCR-10-0825

of HMGB-1 protein on the repair of cisplatin-damaged DNA is accomplished through the acidic domain. Biochemistry 2005;44: 5893–8.

25. Zong W-X, Ditsworth D, Bauer DE, Wang Z-Q, Thompson CB. Alkylating DNA damage stimulates a regulated form of necrotic cell death. Genes Dev 2004;18:1272–82.
26. Arioka H, Nishio K, Ishida T, et al. Enhancement of cisplatin sensitivity in high mobility group 2 cDNA-transfected human lung cancer cells. Cancer Sci 1999;90:108–15.
27. Štros M, Ozaki T, Baèíková A, Kageyama H, Nakagawara A. HMGB1 and HMGB2 cell-specifically down-regulate the p53- and p73-dependent sequence-specific transactivation from the human Bax gene promoter. J Biol Chem 2002;277:7157–64.
28. Völp K, Brezniceanu M-L, Bösser S, et al. Increased expression of high mobility group box 1 (HMGB1) is associated with an elevated level of the antiapoptotic c-IAP2 protein in human colon carcinomas. Gut 2006;55:234–42.
29. Ellerman JE, Brown CK, Vera Md, et al. Masquerader: high mobility group box-1 and cancer. Clin Cancer Res 2007;13:2836–48.
30. Cheng B-Q, Jia C-Q, Liu C-T, et al. Serum high mobility group box chromosomal protein 1 is associated with clinicopathologic features in patients with hepatocellular carcinoma. Dig Liver Dis 2008;40:446–52.
31. Degryse B, Bonaldi T, Scaffidi P, et al. The high mobility group (HMG) boxes of the nuclear protein HMG1 induce chemotaxis and cytoskeleton reorganization in rat smooth muscle cells. J Cell Biol 2001;152: 1197–206.
32. Fages C, Nolo R, Huttunen HJ, Eskelinen E-L, Rauvala H. Regulation of cell migration by amphoterin. J Cell Sci 2000;113: 611–20.
33. Kostova N, Zlateva S, Ugrinova I, Pasheva E. The expression of HMGB1 protein and its receptor RAGE in human malignant tumors. Mol Cell Biochem 2010;337:251–8.
34. Pusterla T, Marchis Fd, Palumbo R, Bianchi ME. High mobility group B2 is secreted by myeloid cells and has mitogenic and chemoattractant activities similar to high mobility group B1. Autoimmunity 2009; 42:308–10.
35. Boonyaratanakornkit V, Melvin V, Prendergast P, et al. High-mobility group chromatin proteins 1 and 2 functionally interact with steroid hormone receptors to enhance their DNA binding *in vitro* and transcriptional activity in mammalian cells. Mol Cell Biol 1998;18: 4471–87.
36. Le X-F, Lammayot A, Gold D, et al. Genes affecting the cell cycle, growth, maintenance, and drug sensitivity are preferentially regulated by anti-HER2 antibody through phosphatidylinositol 3-kinase-AKT signaling. J Biol Chem 2005;280:2092–104.
37. Taniguchi N, Caramés B, Kawakami Y, Amendt BA, Komiya S, Lotz M. Chromatin protein HMGB2 regulates articular cartilage surface maintenance via β-catenin pathway. Proc Natl Acad Sci U S A 2009;106:16817–22.

AACR American Association for Cancer Research

Clinical Cancer Research

Overexpression of High-Mobility Group Box 2 Is Associated with Tumor Aggressiveness and Prognosis of Hepatocellular Carcinoma

Jung-Hee Kwon, Jongmin Kim, Jin Young Park, et al.

Clin Cancer Res 2010;16:5511-5521. Published OnlineFirst September 17, 2010.